Preparation and characterization of molybdenum-doped ReS_2 single crystals

2002 J. Phys.: Condens. Matter 14 4737

(http://iopscience.iop.org/0953-8984/14/18/308)

INSTITUTE OF PHYSICS PUBLISHING JOURNAL OF PHYSICS: CONDENSED MATTER

J. Phys.: Condens. Matter **14** (2002) 4737–4746 PII: S0953-8984(02)31297-9

Preparation and characterization of molybdenum-doped ReS_2 single crystals

P C Yen[1], M J Chen[1], Y S Huang[1,4], C H Ho[2] and K K Tiong[3]

[1] Department of Electronic Engineering, National Taiwan University of Science and Technology, Taipei 106, Taiwan, Republic of China
[2] Department of Electronic Engineering, Kuang Wu Institute of Technology, Peitou, Taipei 112, Taiwan, Republic of China
[3] Department of Electrical Engineering, National Taiwan Ocean University, Keelung 202, Taiwan, Republic of China

Received 27 November 2001, in final form 14 March 2002
Published 26 April 2002
Online at stacks.iop.org/JPhysCM/14/4737

Abstract

Single crystals of Mo-doped rhenium disulphide (ReS_2) have been grown by the chemical vapour transport method using bromine as a transporting agent. Single-crystalline platelets of up to 5×5 mm^2 surface area and 100 μm in thickness were obtained. From the x-ray diffraction patterns, the doped crystals are found to crystallize in the triclinic layered structure. The Hall coefficient measurement indicates that the samples are n-type in nature. The doping effects of the material are characterized by temperature-dependent conductivity, optical absorption and piezoreflectance measurements. The activation energies for the impurity carriers increase with doping. The indirect energy gap of the doped sample shows a slight red-shift. The direct band-edge excitonic transition energies remain unchanged, while the broadening parameter of the excitonic transition features increases due to impurity scattering.

1. Introduction

Rhenium disulphide (ReS_2) is a diamagnetic indirect semiconductor belonging to the family of transition-metal dichalcogenides crystallized in a distorted layered structure of triclinic symmetry [1, 2]. It is an object of considerable interest because of its highly anisotropic electrical, optical and mechanical properties [3] and its possible applications as a sulphur-tolerant hydrogenation and hydrodesulphurization catalyst [4], as a promising solar-cell material in electrochemical cells [5,6] and as a material for fabrication of polarization-sensitive photodetectors [7] in the visible wavelength region. Owing to the potential technological applications of the material, various efforts have been devoted to achieving a theoretical and experimental understanding of the solid-state properties of ReS_2 [8–10]. It is known that

[4] Author to whom any correspondence should be addressed.

0953-8984/02/184737+10$30.00

doping of semiconductors leads to a change in their physical properties. However, only a few works concerning the effect of dopants on the electrical and optical properties of ReS_2 have been reported.

In this paper we report the growth and characterization of Mo-doped ReS_2 single crystals. The motivation for choosing molybdenum (Mo) as the doping agent comes from our earlier efforts in a study of Re-doped MoS_2, which resulted in an increase in the electrical conductivity as well as a structural change from 2H- to 3R-MoS_2 [15]. However, the extremely low-solubility range of the two compounds (ReS_2 and MoS_2) restricted the growth of higher-concentration Re-doped MoS_2 single crystals for further investigation. Therefore it would be of fundamental interest to look at the 'inverse' system consisting of Mo-doped ReS_2. Single crystals of ReS_2 doped with Mo were grown by the chemical vapour transport method using bromine as a transporting agent. The crystal structure was analysed by means of x-ray diffraction patterns. Temperature-dependent electrical conductivity measurements along and perpendicular to the *b*-axis in the van der Waals plane were carried out in the temperature range from 20 to 300 K. The indirect band-edge transitions and direct band-edge excitonic transitions were studied by means of polarization-dependent transmittance and piezoreflectance (PzR), respectively. For comparison purpose the same measurements for the undoped ReS_2 single crystals grown by us previously were also included [8–10]. The effects of the dopant (Mo) on the electrical transport and optical properties were analysed and discussed.

2. Crystal growth

Single crystals of the representative system $Mo_xRe_{1-x}S_2$ were grown using the chemical vapour transport method [11, 12] with Br_2 as a transport agent. The total charge used in each growth experiment was about 10 g. The stoichiometrically determined weight of the doping material (Mo) was added in the hope that it would be transported at a rate similar to that for rhenium. Prior to the crystal growth, a quartz ampoule (22 mm OD, 17 mm ID, 20 cm length) containing Br_2 ($\sim$5 mg cm^{-3}) and the elements (Mo, 99.99% pure; Re, 99.99%; S, 99.999%) was cooled with liquid nitrogen, evacuated to 10^{-6} Torr and sealed. It was shaken well to achieve uniform mixing of the powder. The ampoule was placed in a three-zone furnace and the charge prereacted for 24 h at 850 °C with the growth zone at 950 °C, preventing the transport of the product. The temperature of the furnace was increased slowly. The slow heating was necessary to avoid any possibility of explosion due to the exothermic reaction between the elements. The furnace was then equilibrated to give a constant temperature across the reaction tube, and was programmed over 24 h to produce the temperature gradient at which single-crystal growth took place. A temperature gradient of approximately 2 °C cm^{-1} with the temperature varying from 1040 to 1000 °C over a reaction length of 20 cm gives optimal conditions for the crystallization of the samples. After 360 h, the furnace was allowed to cool down slowly (40 °C h^{-1}) to about 200 °C. The ampoule was then removed and wet tissues applied rapidly to the end away from the crystals to condense the Br_2 vapour. When the ampoule reached room temperature, it was opened and the crystals removed. The crystals were then rinsed with acetone and deionized water. Single-crystalline platelets up to 5×5 mm^2 in surface area and 100 μm in thickness were obtained. ReS_2 crystallizes in a distorted C6 structure [1, 2], while MoS_2 crystallizes with 2H or 3R structure [1], so only a small solubility range is to be expected. It was found that a 4% nominal doping of ReS_2 prevented the growth of single crystals.

Auger electron spectroscopy (AES) and energy-dispersive x-ray (EDX) analysis were utilized for the estimation of the Mo composition x. The AES detection limits ($\sim$0.1%) can vary appreciably from element to element and be influenced by the beam current and analysis time, making quantitative AES analysis difficult [13]. Nevertheless, AES indicates

the presence of a small quantity of Mo and the average concentration of Mo in the sample crystals tends to vary from crystal to crystal. The EDX analysis is sensitive to concentration of $x \geqslant 0.01$ [13]. However, since no Mo is being detected by the EDX analysis, we conclude that the concentration of Mo in the ReS_2 crystals must be extremely low. The two transition metals are most probably chemically transported at different rates and most of the doping material must remain in the untransported residual charge. Considerable discrepancy exists between the nominal doping ratios and those determined by means of AES and EDX. The nominal concentration x will be much larger than the actual one. Because of the immiscibility of the two compounds (MoS_2 and ReS_2), the formation of the ternary system $Mo_xRe_{1-x}S_2$ is not very likely and the name is used only symbolically to represent the intended amount of molybdenum in the growth of doped ReS_2. The Hall coefficient measurement indicates that the doped samples are n-type in nature and the Hall mobility is found to be around 20 $cm^2\ V^{-1}\ s^{-1}$ at room temperature.

3. Characterization

3.1. X-ray diffraction

For x-ray diffraction studies, several small crystals from batches of $Mo_xRe_{1-x}S_2$ with nominal concentration $x = 0.01$ were finely ground with a mixture of glass powder and the x-ray powder patterns were taken and recorded by means of a slow-moving radiation detector. Cu Kα radiation ($\lambda = 1.542$ Å) was employed and a silicon standard was used for the experimental calibration. Structural parameters with reasonable standard errors ($\pm 0.01\%$) were determined by the least-squares fitting of Jandel Sigmaplot mathematical software [14]. The lattice parameters a, b, c, α, β and γ were determined to be 6.450 ± 0.005 Å, 6.390 ± 0.005 Å, 6.403 ± 0.005 Å, $105.49 \pm 0.05^\circ$, $91.32 \pm 0.05^\circ$ and $119.03 \pm 0.05^\circ$, respectively. These numbers are similar to those for the undoped ReS_2 and consistent with those previously reported [2]. The result indicates that the structure of the Mo-doped ReS_2 remains unchanged, which is different from the previous report for Re-doped MoS_2 single crystals [15] that the crystal structure changed from 2H to 3R with a small incorporation of rhenium into the MoS_2 single crystals.

3.2. Temperature-dependent electrical conductivity

The temperature dependence of the electrical conductivity was studied between 20 and 300 K by using a four-probe potentiometric technique. The selected sample was cut into a rectangular shape. Electrical connections to the crystal were made by means of four parallel gold wires (parallel or perpendicular to the b-axis in the van der Waals plane) laid across the basal surface of the thin crystal and attached to the crystal surface by means of conducting silver paint. The wires near each end of the rectangular crystal acted as current leads, while the two contact wires on either side of the central line were used to measure the potential difference V in the crystal. The potential difference V measured by a sensitive potentiometer is taken to be the average value obtained on reversing the current through the sample. Shown in figure 1 are the crystal morphology and the crystal structure in the van der Waals plane of Mo-doped ReS_2. The as-grown thin dark lines in the crystal plane correspond to the orientation of the b-axis. The b- and a-axes are the shortest and second-shortest axes in the basal plane with the b-axis parallel to the Re-cluster chains and corresponds to the longest edge of the plate.

The results of the temperature-dependent conductivity measurements along and perpendicular to the b-axis of the Mo-doped ReS_2 (with the nominal Mo concentration

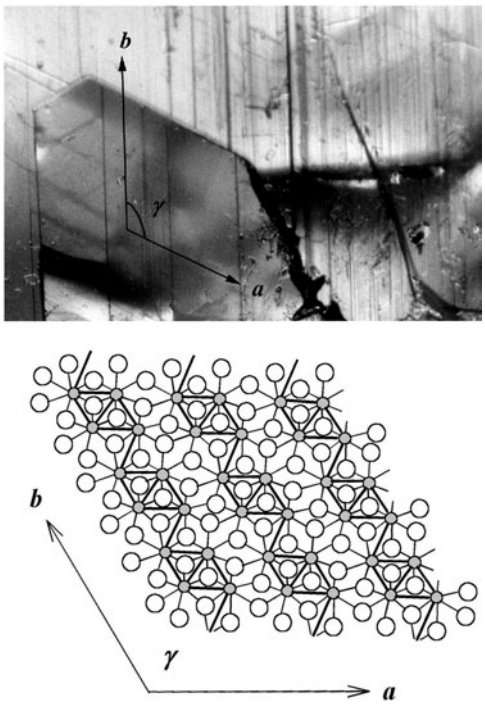

Figure 1. The crystal morphology and crystal structure in the van der Waals plane of Mo-doped ReS_2 single crystals. The as-grown thin dark lines in the crystal plane correspond to the orientation of the *b*-axis.

$x = 0.01$), denoted as ReS_2:Mo, and undoped ReS_2 single crystals are shown in figure 2. The results show the electrical anisotropy in the van der Waals plane of the samples with the conductivity along the *b*-axis, $\sigma_{\|b}$ larger than that of the perpendicular one, $\sigma_{\perp b}$. The larger value of the conductivity parallel to the *b*-axis is related to the strongest bonding force of the samples, which exists along the crystal orientation direction of the Re-cluster chains. The conductivity of the doped sample is found to be much lower than that of the undoped one, which is quite different to the usual increase of conductivity due to doping. The anomalous temperature-dependent conductivity of the doped samples will be discussed in the following. From figure 2, the conductivity of the samples increases as the temperature is raised up to 300 K. The increase of the conductivity in this temperature range is attributed to the ionization effect of impurities. The temperature dependence of the conductivity in the range ∼250–300 K can be expressed as [16]

$$\sigma(T) = \sigma_0 \exp(-E_a/kT) \tag{1}$$

where E_a is the carrier activation energy. The $\ln\sigma$ versus $1000/T$ graph (figure 2) shows the linear region where the slopes yield carrier activation energies for the samples. The active energies determined are summarized in table 1. The results show that the activation energy of the doped sample (∼206 meV) is much higher than that of the undoped one (∼177 meV) [17]. This result, together with the observation of lowering of conductivity, shows that the incorporation of Mo into ReS_2 has formed deep impurity levels in the host crystals.

Table 1. Summary of the experiment results: polarization-dependent electrical conductivity, optical absorption and piezoreflectance measurements for Mo-doped ReS_2 (ReS_2:Mo) and ReS_2 single crystals.

Method		Conductivity	Absorption		Piezoreflectance				
			Indirect band edge		Direct band-edge excitons				
					Excitonic transition energy (eV)			Broadening parameter (meV)	
Parameter: Material		Activation energy E_a (meV)	Energy gap E_g (eV)	Phonon energy E_p (meV)		E_1^{ex}	E_2^{ex}	Γ_1	Γ_2
ReS_2:Mo	$\sigma_\parallel$	202 ± 10	$\boldsymbol{E} \parallel \boldsymbol{b}$ 1.31 ± 0.02	32 ± 5	30 K	1.554 ± 0.001	1.585 ± 0.001	8 ± 1	7 ± 1
	$\sigma_\perp$	210 ± 10	$\boldsymbol{E} \perp \boldsymbol{b}$ 1.33 ± 0.02	23 ± 5	300 K	1.485 ± 0.002	1.516 ± 0.002	35 ± 2	23 ± 2
ReS_2	$\sigma_\parallel$	174 ± 10	$\boldsymbol{E} \parallel \boldsymbol{b}$ 1.35 ± 0.02	30 ± 5	30 K	1.554 ± 0.001	1.584 ± 0.001	6 ± 1	6 ± 1
	$\sigma_\perp$	179 ± 10	$\boldsymbol{E} \perp \boldsymbol{b}$ 1.38 ± 0.02	26 ± 5	300 K	1.484 ± 0.002	1.518 ± 0.002	31 ± 2	21 ± 2

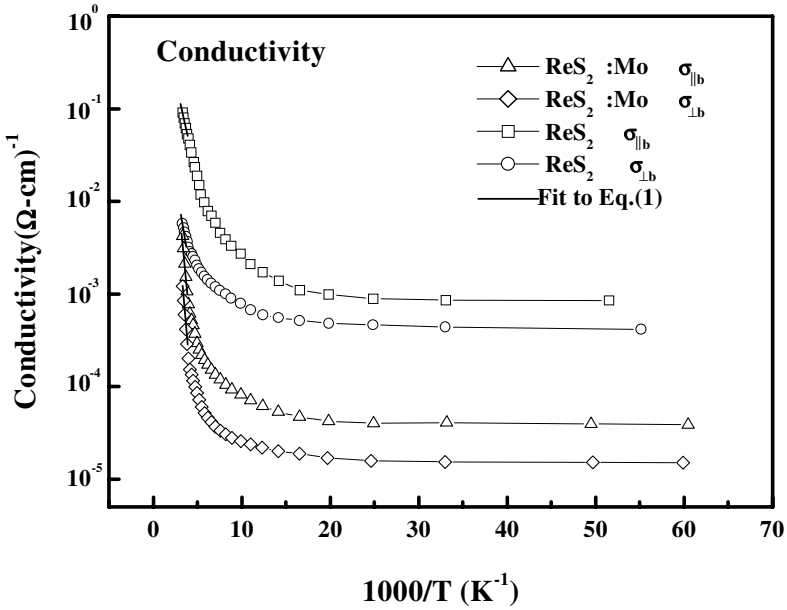

Figure 2. The temperature-dependent conductivity along and perpendicular to the *b*-axis of the Mo-doped ReS_2 (ReS_2:Mo) and undoped ReS_2 single crystals. The slopes of $\ln\sigma$ versus $1000/T$ yield carrier activation energies for the samples.

3.3. Optical absorption

The indirect band-edge transitions of the undoped and Mo-doped ReS_2 (with the nominal Mo concentration $x = 0.01$) are studied by means of polarization-dependent transmittance. From polarization-dependent optical reflectivity and transmittance measurements, the absorption coefficient α of the sample crystals can be determined by using the relation [18]

$$T_r = \frac{(1-R)^2\exp(-\alpha d)}{1-R^2\exp(-2\alpha d)} \tag{2}$$

where T_r represents the transmission coefficient, R is the reflectivity and d is the sample thickness. The reflectivity measurements were done on as-grown surfaces and compared against an evaporated gold mirror. The variation of the absorption coefficient of Mo-doped and undoped ReS_2 with photon energy is presented in figure 3. The open-diamond (open-circle) curve in figure 3 corresponds to the $\boldsymbol{E} \parallel \boldsymbol{b}$ polarization and the open-triangle (open-square) curve represents $\boldsymbol{E} \perp \boldsymbol{b}$ polarization for ReS_2:Mo (ReS_2). The small oscillations below the absorption edge attributed to interference effects are frequently observed for thin layered crystals [19]. The polarization dependence of the absorption curves provides conclusive evidence that the two optical absorption edges are associated with the interband transitions from different origins. Analysis of the polarization-dependent experimental data on the absorption coefficient α shows an indirect allowed transition for the materials.

The experimental points for $(\alpha h\nu)^{1/2}$ versus photon energy, $h\nu$, that are deduced from polarization-dependent absorption measurements for Mo-doped and undoped ReS_2 at 300 K are shown in figure 4. The open diamonds (open circles) and open triangles (open squares) are data points from the $\boldsymbol{E} \parallel \boldsymbol{b}$ and $\boldsymbol{E} \perp \boldsymbol{b}$ polarization measurements, respectively, for ReS_2:Mo (ReS_2) and the solid curves are the least-squares fits to the expression [18]

$$\alpha h\nu = \frac{A(h\nu - E_g + E_p)^2}{\exp(E_p/kT)-1} + \frac{B(h\nu - E_g - E_p)^2}{1-\exp(-E_p/kT)} \tag{3}$$

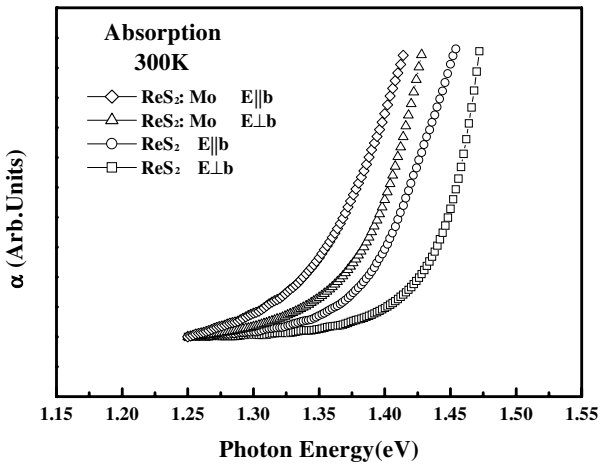

Figure 3. The variation of the absorption coefficient of Mo-doped and undoped ReS_2 with photon energy. The open-diamond (open-circle) curve corresponds to the $\boldsymbol{E} \parallel \boldsymbol{b}$ polarization and the open-triangle (open-square) curve represents $\boldsymbol{E} \perp \boldsymbol{b}$ polarization for ReS_2:Mo (ReS_2).

where $h\nu$ is the energy of the incident photon, E_g the band gap, E_p the energy of the phonon assisting the transitions, and A and B are constants. The first term on the right-hand side of equation (3) corresponds to absorption of a photon and a phonon, whereas the second term corresponds to absorption of a photon and emission of a phonon and contributes only when $h\nu \geqslant E_g + E_p$. To evaluate the band gap E_g and phonon energy E_p with the use of equation (3), the background absorption is subtracted out. The results indicate that the Mo-doped and undoped ReS_2 samples are indirect semiconductor, in which $\boldsymbol{E} \parallel \boldsymbol{b}$ polarization exhibits a smaller band gap and a single phonon makes an important contribution in assisting the indirect transitions. The non-uniform thickness and non-smooth sample surface will tend to cause the angles of incidence to deviate from the normal direction, resulting in some variations in the absorption spectra. Differing values of E_g and E_p could be obtained by fitting a different energy range; thus errors of the order of ± 0.02 eV and ± 5 meV can be deduced for the estimates of E_g and E_p, respectively. The fitted values of the energy gaps and phonon energy of the sample crystals are summarized in table 1. The results show that incorporation of small amounts of molybdenum into ReS_2 shifts the absorption edge about 0.04 eV towards the lower-energy region. The physical origin of the shift may come from the existence of n-type impurity, which in general will contribute to the absorption near the band tail. This point requires further verification and more work is needed.

3.4. Piezoreflectance

The direct band-edge excitonic transitions are studied by means of polarization-dependent PzR at 30 and 300 K. The unpolarized, $\boldsymbol{E} \parallel \boldsymbol{b}$ polarization and $\boldsymbol{E} \perp \boldsymbol{b}$ PzR spectra of Mo-doped and undoped ReS_2 in the vicinity of the direct band edge are respectively shown by the open-circle and open-triangle curves at 30 and 300 K in figures 5(a)–(c). The two dominant structures located between 1.54 and 1.6 eV (figure 5(a), 30 K) are associated with band-edge excitonic transitions from different origins and were previously assigned as E_1^{ex} and E_2^{ex} [8]. As shown in figure 5(b), the E_2^{ex}-feature is absent in $\boldsymbol{E} \parallel \boldsymbol{b}$ polarization while the E_1^{ex}-feature disappears in $\boldsymbol{E} \perp \boldsymbol{b}$ polarization (see figure 5(c)). We have fitted the polarized curves to a functional form appropriate for excitonic transitions that can be expressed as a Lorentzian line-shape function

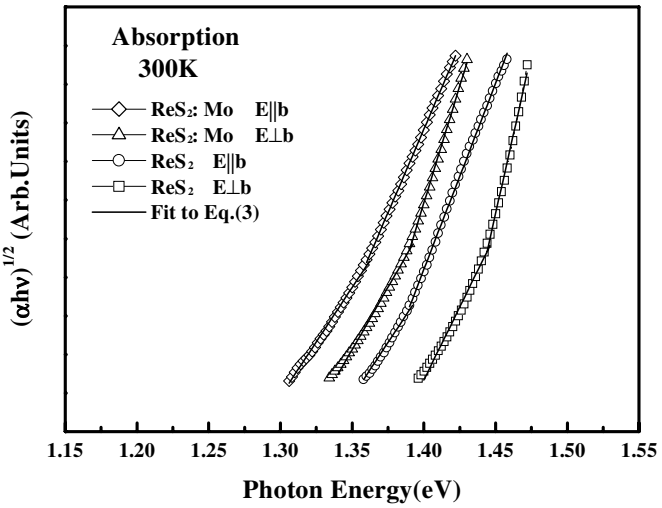

Figure 4. The experimental points for $(\alpha h\nu)^{1/2}$ versus photon energy, $h\nu$, deduced from polarization-dependent absorption measurements for Mo-doped and undoped ReS_2 at 300 K. The open diamonds (open circles) and open triangles (open squares) are data points from the $\boldsymbol{E} \parallel \boldsymbol{b}$ and $\boldsymbol{E} \perp \boldsymbol{b}$ polarization measurements, respectively, for ReS_2:Mo (ReS_2) and the solid curves are the least-squares fits to equation (3).

of the form [20]

$$\frac{\Delta R}{R} = \mathrm{Re}\sum_{i=1}^{2} A_i \mathrm{e}^{\mathrm{i}\phi_i}(h\nu - E_i^{ex} + \mathrm{i}\Gamma_i^{ex})^{-2} \tag{4}$$

where A_i and ϕ_i are, respectively, the amplitude and phase of the line shape, and E_i^{ex} and Γ_i^{ex} are, respectively, the energy and broadening parameter of the band-edge excitonic transitions. Shown by the solid curves in figures 5(a)–(c) are the least-squares fits using equation (4). Arrows under the curves in figures 5(a)–(c) show the peak positions of the two interband excitonic features, E_1^{ex} and E_2^{ex}. The energies and broadening parameters obtained for these features are summarized in table 1. The unpolarized spectrum can be regarded as a random superposition of the spectra with $\boldsymbol{E} \parallel \boldsymbol{b}$ and $\boldsymbol{E} \perp \boldsymbol{b}$ polarizations. The results summarized in table 1 show that the direct band-edge excitonic transition energies are not sensitive to a small concentration of molybdenum doping. Nevertheless the effect of dopant shows up in a slight increase of the broadening parameter of the excitonic features. The increase of the broadening parameter for the Mo-doped sample is mainly due to impurity scattering.

4. Summary

In summary, single crystals of Mo-doped ReS_2 with surface area up to 5×5 mm^2 and 100 μm in thickness have been grown by the chemical vapour transport method using bromine as a transport agent. The effects of doping on the electrical conductivity and optical properties are studied. The results indicate that incorporation of a small amount of molybdenum into ReS_2 has formed deep impurity levels, which caused a lowering of the electrical conductivity. The indirect energy gap of the doped sample shows a red-shift, while the direct band-edge excitonic transition energies remain unchanged. The broadening parameter of the excitonic transition features increases due to impurity scattering.

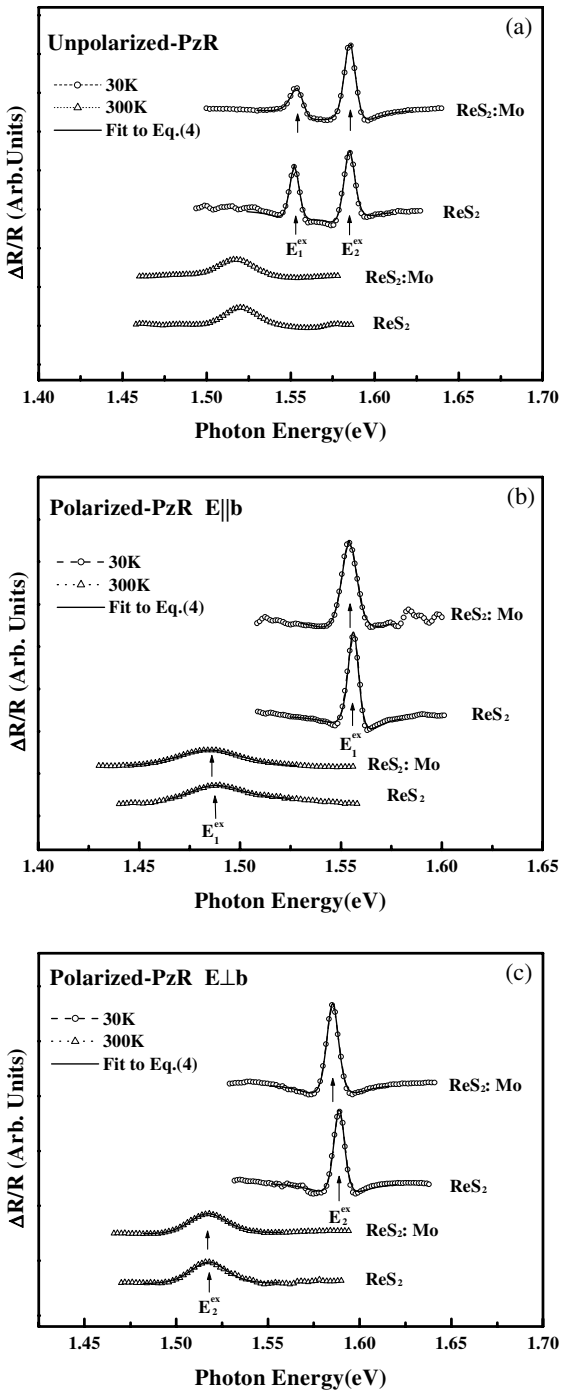

Figure 5. (a) The unpolarized, (b) $\boldsymbol{E} \parallel \boldsymbol{b}$ polarization and (c) $\boldsymbol{E} \perp \boldsymbol{b}$ PzR spectra of Mo-doped and undoped ReS_2 in the vicinity of direct band edge are respectively shown by the open-circle and open-triangle curves at 30 and 300 K. The solid curves are the least-squares fits using equation (4). Arrows under the curves show the peak positions of the two interband excitonic features, E_1^{ex} and E_2^{ex}, respectively.

Acknowledgments

The authors P C Yen, M J Chen and Y S Huang would like to acknowledge the support of the National Science Council of the Republic of China under project no 90-2112-M-011-001. C H Ho and K K Tiong acknowledge the support of the National Science Council of the Republic of China under project no NSC89-2112-M-019-006.

References

[1] Wilson J A and Yoffe A D 1969 *Adv. Phys.* **18** 193
[2] Wildervanck J C and Jellinek F 1971 *J. Less-Common Met.* **24** 73
[3] Ho C H, Huang Y S, Tiong K K and Liao P C 1999 *J. Phys.: Condens. Matter* **11** 5367
[4] Kelty S P, Ruppert A F, Chianelli R R, Ren J and Whangbo M-H 1994 *J. Am. Chem. Soc.* **116** 7857
[5] Koffyberg F P, Dwight K and Wold A 1979 *Solid State Commun.* **30** 433
[6] Wheeler B L, Leland J K and Bard A J 1986 *J. Electrochem. Soc.* **133** 358
[7] Friemelt K, Lux-Steiner M-Ch and Bucher E 1993 *J. Appl. Phys.* **74** 5266
[8] Ho C H, Liao P C, Huang Y S and Tiong K K 1997 *Phys. Rev.* B **55** 15 608
[9] Ho C H, Huang Y S, Chen J L, Dann T E and Tiong K K 1999 *Phys. Rev.* B **60** 15 766
[10] Ho C H, Huang Y S, Liao P C and Tiong K K 1999 *J. Phys. Chem. Solids* **60** 1797
[11] Schäffer H 1964 *Chemical Transport Reactions* (New York: Academic)
[12] Huang Y S 1984 *Chin. J. Phys.* **22** 43
[13] Schroder D K 1998 *Semiconductor Material and Device Characterization* 2nd edn (New York: Wiley) p 671 ch 10
[14] *Sigmaplot Scientific Graph System* Version 1.01 (Jandel Corporation)
[15] Tiong K K, Liao P C, Ho C H and Huang Y S 1999 *J. Cryst. Growth* **205** 543
[16] Mahalaway S H and Evans B L 1977 *Phys. Status Solidi* b **79** 713
[17] Tiong K K, Ho C H and Huang Y S 1999 *Solid State Commun.* **111** 635
[18] Pankove J I 1975 *Optical Processes in Semiconductors* (New York: Dover)
[19] Kam K K, Chang C L and Lynch D W 1984 *J. Phys. C: Solid State Phys.* **17** 4031
[20] Pollak F H and Shen H 1993 *Mater. Sci. Eng.* R **10** 275